Hindawi
Advances in Materials Science and Engineering
Volume 2021, Article ID 7663348, 10 pages
https://doi.org/10.1155/2021/7663348

Research Article

Artificial Intelligence to Analyze the Performance of the Ceramic-Coated Diesel Engine Using Digital Filter Optimization

P. Nirmala,[1] **G. Ramkumar**,[1] **Satyajeet Sahoo**,[2] **G. Anitha**,[1] **S. Ramesh**,[3] **S. Agnes Shifani**,[4] **and Agegnehu Shara Shata**[5]

[1]*Department of Electronics and Communication Engineering, Saveetha School of Engineering, SIMATS, Chennai 602 105, Tamil Nadu, India*
[2]*Department of Electronics and Communication Engineering, Vignan's Foundation for Science, Technology and Research (Deemed to be University), Vadlamudi Guntur, Andra Pradesh-522213, India*
[3]*Department of Electronics and Communication Engineering, Sri Shakthi Institute of Engineering and Technology, Coimbatore-641062, Tamilnadu, India*
[4]*Department of Electronics and Communication Engineering, Jeppiaar Maamallan Engineering College, Chennai, Tamilnadu, India*
[5]*Faculty of Mechanical Engineering, Arba Minch Institute of Technology, Arba Minch, Ethiopia*

Correspondence should be addressed to P. Nirmala; nirmalajai@gmail.com and Agegnehu Shara Shata; agegnehu.shara@amu.edu.et

Received 6 August 2021; Accepted 31 August 2021; Published 9 September 2021

Academic Editor: P Ganeshan

The completeness of oil goods activates the barriers of lack of goods, inequality in the society, and surroundings impoverishment. Avoiding their use overnight and switching to clean electric motors are a challenge. Under all these conditions, researchers can launch their research on alternative fuels for a preeminent solution. Oxygenated fuel additives and thermal barrier coating (TBC) applications are essential to decrease the emission levels of exhaust and improve the performance of the vehicle. The main objective of this research is to analyze the performance of the ceramic-coated diesel engine. The ceramic particles use polymer coating to enhance the functionality and durability. Optimum outcomes are determined using Taguchi method. The impacts of various casting parameters of composites have been examined in detail. PSO-GA (Particle Swarm Optimization and Genetic Algorithm) is utilized to analyze the performance. Using an artificial neural network (ANN), the performance of diesel engine is examined to reduce time, cost, and experimental repetition. Thus, by using the artificial intelligence, the performance of the ceramic-coated diesel engine is analyzed and the polymeric substance and condition in coating ceramic engine is discussed.

1. Introduction

An enormous opening up of trade abroad and, on the other hand, the increase in emissions towards the impoverishment of the environment has brought attention to the replacement of diesel and gasoline. Oil provides energy for around 90% of transportation and transport, and mandate is growing gradually, particularly in developing countries such as India and China [1]. Our country's home oil stock accounts for only a quarter of total demand, with the remaining demands being satisfied with petroleum products imported from other nations. As a result, the essential steps have been taken to reduce the country's reliance on crude oil imports from other countries. The blends of biofuel are made from fats of veggies and animals and the fatty methyl acid is prepared from biomass. Biofuel is a biodegradable, recreate able fuel that may be used in fuel engines. Despite the fact that biofuel has the ability to reduce net CO_2 emissions, there are two barriers to its widespread adoption as a fossil fuel diesel substitute. As a result, the biofuel adoption strategy is to mix biofuel with fossil fuel diesel fuels, with permissible limits of diesel-biofuel blend compositions determined to safely use biofuel without harming diesel engines and to reduce NOx emissions.

Pores are frequently avoided in ceramic components due to their brittle nature, unlike porous metal and polymer constructions. However, in current decades, the number of submissions needing porous ceramics has been increased, particularly in situations including high temperatures, extensive wear, and corrosive fluids. After drying and pyrolyzing the polymeric model covered in ceramic, it is carefully heated between 3001 and 8001 degrees Celsius. To allow for progressive disintegration and diffusion of the polymeric material, heating rates of less than 11 C/min are required at this step [2]. Allowing pressure to build up in coated spacers is not a good idea. To provide ceramic coatings strong enough to prevent spacer cracking during pyrolysis, binders and plasticizers are added to the initial suspension. Some of the most commonly used binders include colloidal aluminum orthophosphate, potassium and sodium silicates, magnesium orthoborate, hydratable alumina, colloidal silica, polyvinyl butyral with polyethylene glycol as a plasticizer, and polymerizable monomers. The ceramic covering is densified after the polymer plate is removed by sintering in a suitable environment at temperatures ranging from 11001 to 11000 degrees Fahrenheit, depending on the material [3].

Plasma polymerization has been utilized to increase the corrosion and photodegradation resistance of items in a variety of industrial applications. Surface activation in a plasma environment through particle impact or photon radiation enhances monomer molecule deposition and polymerization on the substrate surface, providing a benefit not seen in nonplasma methods [4]. In reciprocating and rotary engines for transportation and stationary power, ceramic coatings have a considerable impact on reducing wear and abrasion failure. When operating temperatures are pushed higher to improve efficiency in these engines, the wear/abrasion problem gets more challenging, because lubrication in high temperature regions becomes increasingly problematic [5].

In automobiles, the IC engine is the major source of power. The piston, cylinder head, and cylinder block are among the many components that make up the engine. The most important components of an IC engine are piston and cylinder head, which is situated between the cylinder head's bottom and the piston. Pollutants are created as a result of combustion [6]. Combustion is the process of burning fuel in the presence of air. Diesel engines are used as the preferred engines for heavy-duty vehicles because of their high performance and low specific fuel consumption. Their use in light-duty vehicles has also increased over the last couple of years. In view of the strict legislation on emission control, statutory limits have become even more stringent. The major pollutants are fumigated, HC, NOx, and the material involved. However, diesel engines became more popular than other engines due to better torque characteristics and fuel economy [7].

2. Related Works

The literature review section of the paper includes the work proposed previously for analyzing the performance of ceramic coating diesel engine.

In the presence of thick layer polymer, acidic solutes have strong relation with zirconia surface [8]. The phosphate in the phase of mobile can reduce these interactions, making the polymer-coated zirconia's small solute retention qualities equivalent to alkyl silane-derivatized silica-based reversed-phase supports. With crude vegetable oil and different injector opening pressures, [9] examined the performance of a diesel engine with a ceramic-coated cylinder head. The performance parameters of the ceramic-coated combustion chamber were measured at various brake mean effective pressures and associated to neat operation of diesel on a conventional engine (CE) and vegetable oil operation at similar operating conditions.

The authors in [10] described that the ethanol can be made by fermenting and distilling biomasses, and it can thus be called a renewable fuel. Using the ethanol fuel CI engine as a Low-Heat-Rejection Engine is one method to improve its efficiency (LHR). The thermal efficiency of the CI engine can be improved in the LHR engine by limiting heat loss to the environment through coolant and exhaust gas. Heat transmission can be reduced by insulating the piston and cylinder walls, as well as covering the piston and cylinder walls with ceramics that can tolerate high temperatures. The low thermal conductivity of the coating materials reduces the heat flow into the piston and hence the heat transfers to the coolant.

Reference [1] discovered that using correlation coefficients, the ANN model can accurately estimate engine exhaust emissions with very low root mean square errors. The ANN method may be utilized precisely to anticipate the performance and internal combustion engines emission as an alternative to traditional modelling techniques, according to this study. The thickness of ceramic material which is about 200 m topcoat has been applied to the piston. Blends have been evaluated at their rated compression ratio under a variety of operational stresses. According to a comparison of engine parameters driven by diesel, mechanical competence progressively increases with a percentile increment of n-butanol in the mix. Using a backpropagation learning approach, the ability of an artificial neural network model to forecast specific fuel consumption and exhaust temperature of a Diesel engine for various injection timings is examined. The results of the experiment and the network were found to be consistent, with a mean absolute relative error of less than 2%. A well-trained neural network model is thought to produce quick and reliable findings, making it a simple tool to utilize in preliminary research for such thermal engineering challenges.

The chemistry of the surface polymer phase differs significantly from that of bulk polymers. The ease with which polymer coatings can be distributed and handled is one of their most appealing features. They can be applied as liquids, similar to paints, and other additives can be added to improve their qualities [6]. The polymer was identified using infrared, Raman spectroscopy, scanning and transmittance electron microscopy, and a dispersibility test. A uniform core-shell structure and a substantial number of acidic sites characterize the manufactured catalysts. More phosphor tungstic acid can be spread on the polymer's surface thanks to the presence of vinyl benzyl chloride in the polymer [11].

3. Methodology

This study investigates the performance of polymer-coated composite diesel engine. The robust Taguchi method and Minitab-16 software were also used in the experiment. Finally, the prediction of tensile strength and hardness of the composites was performed using ANN.

The performance of and emissions characteristics such as load and speed were changed using diesel, cotton seed oil blended with diesel fuel at a ratio of 10% to 20%, and the engine was tested using diesel, cotton seed oil blended with diesel fuel at a ratio of 10% to 20% [12]. The tests make use of Taguchi orthogonal arrays (OA). The OA was selected with the statistical software Minitab'16. OA is used to create the design of experiments (DOE).

In Figure 1, at first, the engine to be analyzed is selected and then the material to be applied is selected. These two are one of the important processes in investigation process. Continuing to this processing, the engine coating is done and after the completion of coating process, the experimental analysis is done and then continuing to this prediction of ANN result is given.

The tests are carried out in a 150 cc Kirloskar multi-fuel driven diesel engine equipped with an eddy current dynamometer and a gas analyzer. The system provides for the measurement of coated engine emission characteristics K. R. Patil and colleagues investigated diesel engine emissions and tested their performance using ISO 8178-C1 and ISO 8178-D2 protocols. CO is detected using a nondispersive infrared (NDIR) sensor, HC is detected using a flame ionization detector (FID), and NOx is detected using a chemiluminescent analyzer. Zircon is usually used to make zirconia ($ZrSiO_4$). Properties of cotton seed oil as shown in Table 1.

The zircon must be treated with NaOH and HCl to convert it to zirconyl chloride, which is then used to make zirconia. The cylinder head and valve surfaces will be coated with the PSZ powder that is currently available. The following procedures are carried out in this. (1) Rust, scale, sand, paint, and other contaminants are removed from the cylinder head and valve surfaces during precleaning and premachining. (2) Using the polymer spraying technique, apply the PSZ powder to the component surfaces up to the appropriate thickness [13]. Grinding, lapping, polishing, and cleaning are examples of final finishing procedures. It is best for internal combustion engines and has excellent corrosion resistance.

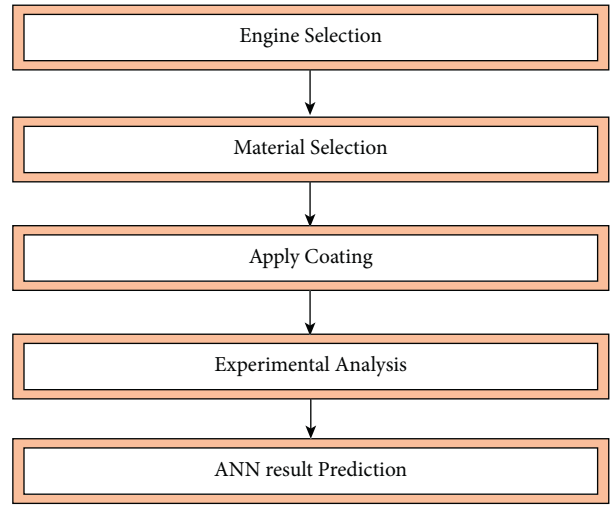

Figure 1: Step-by-step process of investigation process.

Table 1: Properties of cotton seed oil.

S. no.	Parameters	Values
1	Thickness	857 kg/m^3
2	Flash point	198°C
3	Fire point	225°C
4	Greasy value	35 MJ/kg
5	Cetane number	38

4. Polymer Coating

Plasma polymerization has been used to enhance hydrophily or hydrophobicity, erosion or oxidation resistance, and photodegradation resistance in a range of industrial applications. When the surface of a plasma is stimulated by particle impact or photon radiation, deposition and polymerization are accelerated. Monomeric molecules on the surface of the substrate indicate a benefit not seen in loss-free methods. To change the properties of films surface and powder particles, several types of imbalanced cold plasma have been introduced. Using the atmospheric microwave plasma CF_4/Ar or O_2/Ar , contact angle of the polypropylene film was checked. Hydrophobicity is enhanced by polymerization of tetrafluoroethylene on the surface of silica particles in luminescent dielectric barrier discharges.

The plasma processing sample is made up of zirconium ceramic powders with an average particle diameter of 130 nm. Figure 2, plasma Reactor Schematic A quartz jar with an interior diameter of about 80 mm, and a length of about 200 mm makes up the reactor chamber. A 27 MHz RF power supply drives a five-revolutions-per-minute RF antenna [7] that bypasses the chamber to accomplish a decent sign of at least 60% of the Fresnel zone. In numerous down-to-earth settings, transceivers might work with a lower radio wire stature, yet the higher the better. There is additionally a compromise between the receiving wire stature and the measure of RF link expected to range the handset to the radio wire. The sample holder and zirconia powders are dispersed throughout the center of the substrate surface; hence, a glass substrate is used in the chamber. After being fully blended, nitrogen-diluted ethylene is fed into the reactor chamber. With a mass flow control, the mixture ratio is changed by altering the flow rate of each gas. An empty pressure gauge is used to check the overall gas pressure [14]. Inductively coupled C_2H_4/N_2 discharges deposit a narrow polymer coating on the surface of ceramic nano-zirconia particles. Transmission electron microscopy was used to evaluate plasma-treated specimens (TEM). This means that zirconium nanoparticles cover the whole surface of a 5 nm thick polymer film. The film presents the chemical structure of a long chain of quasi-polyethylene hydrocarbons

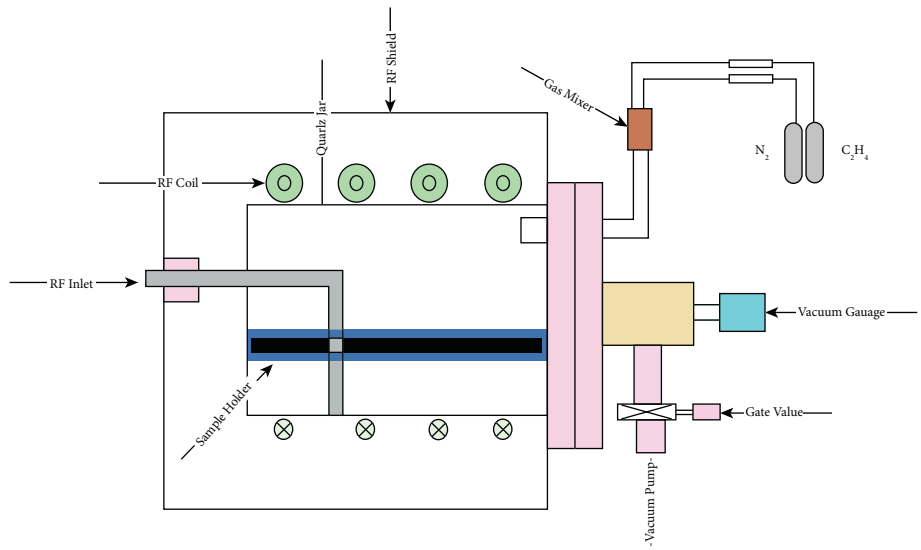

Figure 2: Schematic plasma reactor.

examined by X-ray photoelectric spectroscopy (XPS). This low-temperature dry surface treatment approach for ceramic nano particles is combined with fluidized bed technology. Plasma polymerization could be improved to aid in the synthesis of novel ceramics and improve the technological process [14].

As a plasma processing sample, zirconium ceramic powders with an average particle diameter of 130 nm were used. Figure 2 depicts the plasma reactor schematic. A quartz jar with an interior diameter of roughly 80 mm and a length of 200 mm makes up the reactor chamber [15]. A 27 MHz RF power supply drives a turn 5 RF coil that bypasses the chamber. A glass substrate is used as the specimen holder in the chamber, with zirconia powders scattered in the middle of the surface. After being fully blended, nitrogen-diluted ethylene is fed into the reactor slot. With a mass flow regulator, the blending rate is changed by altering the flow rate of each gas. A vacuum pressure gauge regulates the total pressure of the gas. After plasma treatment, the layer of powders that is the furthest from thin is taken as a sample. TEM (Hitachi, H-800) and XPS are used to analyze the shape and content of the polymeric covering (Perkin-Elmer, PHI-5300 ESCA). Within the XPS system, the radiation source is the Al Ka s1486.6 eVd line. The reading acquisition's passing energy is 100 eV, while the detail acquisition's is 25 eV, with resolutions of 2 and 0.5 eV, respectively.

4.1. Polymer-Coated Zirconia Preparation. Stable zirconia-based reversed phases were generated by depositing and crosslinking polymers on the zirconia surface. Reverse phase is generated by depositing stable zirconia and polymers crosslinked on the zirconia surface. Properties of polymer zirconium material are listed in Table 2.

Aside from stability, polymer-coated reversed phases have the advantage of being able to create materials with a wide range of carbon loading, regardless of the inhabitants of sensitive sites on the external or the firmness of surface

Table 2: Properties of polymer zirconium material.

S. no.	Parameters	Values
1	Tensile strength	225–540 N/mm^2
2	0.2% proof strength	100–440 N/mm^2
3	Elongation	5–35%
4	Hardness (HV)	55–175
5	Electrical conductivity	80% IAC
6	Thermal conductivity	300 W/moK
7	Melting point	1080°C

bonds. By varying the amount of polybutadiene applied to the support, the quantity of carbon on the support surface can be changed by an order of magnitude [16]. When looking at the carbon analysis, it is critical to examine the surface area of the zirconia supports. When standardized to the support surface area, these values cover a wide range of carbon loads, including typical commercial salivated carbon loads. The carbon analysis data obtained on dissimilar zirconia with the same amount of polybutadiene agrees, indicating that the modification process is repeatable under the conditions stated above, as evidenced by the carbon analysis data obtained.

5. Coated Piston

The design for heat distribution for the thermal inquiry in steady state was simulated using ANSYS. An uncoated piston (without alteration) was found to have a temperature range of 350°C to 313.97°C, with a high of 352°C and a low of 313.96°C. The temperature 355°C and 323.85°C were discovered to be the maximum and lowest temperatures for an altered piston (at top surface of ceramic coat). The heat flow of uncoated and coated pistons may also be seen. Based on the aforementioned steady-state thermal investigation, the plasma spray technique was chosen as a thermal spray coating technique to apply the ceramic coating to the piston with a thickness of 200 m topcoat. The medium coated is heated to a molten state,

causing it to strike the membrane surface and instantly cool, forming a coating. This study proposes a ceramic-coated piston for testing biofuels in order to decrease the essential amount of gas pollution emitted by the engine.

Transesterification has been chosen as a filtration strategy for the production of pure biofuel, which should be followed by the esterification procedure. In this case, the oils of *Pongamia pinnata* and *Calophyllum inophyllum* contain a lot of free lipids. The raw sample was heated and then stirred with the addition of NaOH as a methanol and base catalyst. After a chemical reaction and isolation by water washing, the gravitational technique has traditionally been used to isolate the glycerol content of biofuel. These methyl esters were combined with pure diesel in various volume proportions (P10, P20, C10, and C20) with a magnetic agitator for biodiesel preparation procedure as shown in Figure 3.

These samples are blended with an additive (butyl alcohol) in various probabilities ranging from 6% to 12% in volume terms with a 6% interval once more. Because its high burn rates, n-butanol was used as an addition (oxygenate) in this investigation and can rapidly react with diesel. As a result, it appears to be able to sustain combustion in the presence of sufficient oxygen [16]. Before engine testing, the parameters of all mixes are measured with various equipment and are listed in Table 3.

The experiment is carried out on a single cylinder that has been cooled with water four times and injected directly. To apply the load, the CI motor has a ceramic-coated plunger with an eddy current dynamometer. An upper layer of 200 m of alumina was used as a ceramic substance to coat the piston. A low-heat-emitting engine is a compression-ignition (IC) engine having its piston covered in any ceramic material, resulting in minimal heat loss. This redesigned engine is gaining important in today's globe due to growing fuel prices and environmental devastation because it releases fewer emissions [17]. It had a lot of features, including the ability to measure combustion pressure and crank angle. There is a place where you can measure airflow and fuel flow, as well as temperatures and other things. The calorimeter's water flow and the cooling water flow are both measured using Rotameters. To evaluate computerized performance, a flexible set of motors has been added. In computerized mode, a layout allows for the measurement of fuel injection pressure at the nozzle.

6. PSO-GA Algorithm

When PSO and GA are combined, the exploring powers of GA are combined with the exploitation abilities of PSO. In this study, a novel combination of PSO and GA was applied, in which PSO and GA were run in order at each iteration with a small population. PSO for N probable solutions is used at the start of each iteration. Following PSO, the best n solutions are given to a GA procedure, which is based on fitness value. The GA operator pairs these solutions at random while simultaneously applying a mutation to a randomly chosen offspring, which is then brought back to PSO in the following iteration. To reduce dynamometer time, a small population N is desired. In order to reduce time to convergence in conventional benchmark testing, the optimal population size was found to be 8 in the interval [18]. For the sake of simplicity, N and n are both set to 4. The GA mutation rate, as well as the PSO constants C1 and C2, can be found. An objective function was constructed to evaluate each trial's fitness based on the cumulative fitness of five variables in order to optimize several objectives at once for both PSO-GA and ABC. CO, HC, NOx, and PM emissions specific to brakes (g/kW-h) were fed into the objective function and fuel consumption.

7. Taguchi Orthogonal Design

Taguchi method has been effectively employed among the optimization techniques for optimizing the process parameter for a simple and robust procedure. There are three alternative average square deviations estimated for the signal-to-noise ratio according to Taguchi's design objectives: better-the-nominal, better-the-large, and better-the-small. The goal of the study is to reduce warpage and shrinkage. The minimum rate of shrinkage and warpage must be achieved; therefore, the S/N ratio of the smaller-the-better formula must be chosen for optimizing the parameter rate, and so the combination is attained. Orthogonal array design of experiment with various types of fuels is listed in Table 4.

8. Artificial Neural Network

An ANN model can oblige different information factors to anticipate numerous yield factors. It contrasts from ordinary displaying approaches in capacity to find out about the framework can be demonstrated without earlier information on the cycle connections. The forecast by an all-around prepared ANN is typically a lot quicker than the ordinary reproduction programs or numerical models as no extensive iterative computations are expected to address differential conditions utilizing mathematical techniques, yet the determination of a fitting neural organization geography is significant as far as model exactness and model straightforwardness [18]. Notwithstanding the dynamic exportation of oil, the public authority actually needs to import an enormous measure of raw petroleum to satisfy neighborhood interest. A temperamental uncontrolled oil value prompts high government consumption in the spending plan, because of the strategy of exceptionally financed fuel for the neighborhood market later on.

The ANN model is shown in Figure 4. The back-propagation (BP) learning technique is used in this work among the several types of ANN algorithms available. In order to train and evaluate neural networks, the target and input data patterns are required. The existing dataset was separated into two sets while creating an ANN model [19], one for training the network and the other for testing the network's generalization capabilities. The user does not need to know any technical specifics of neural networks because they operate in a "black box" fashion. They are capable of determining the relationship between the input and output. Weights are adjusted to reduce the discrepancy among the network output and the real value, and the network is given

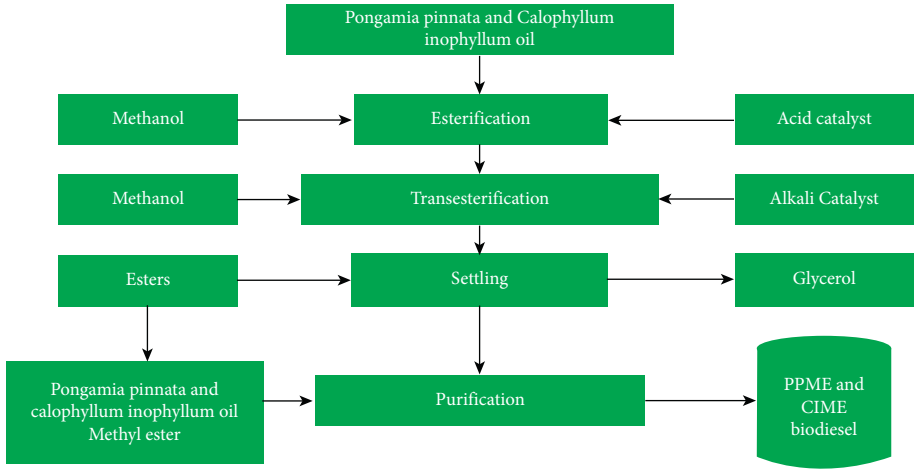

Figure 3: Procedure of biodiesel preparation.

Table 3: Tested sample fuel properties.

Model	Density (kg/m^3)	Gaudy point (°C)	Heating point (°C)	Thickness (cSt)	Calorific value (kJ/Kg)
D100	831	57	65	3.22	42505
P100	899.7	166	180	2.48	35667
C100	897.8	157	166	2.83	35088
P1B6	850	60	69	3.12	41252
P10B12	853	61	71	3.16	40699
P20B6	857	63	74	3.21	40616
P20B12	859	57	75	3.23	40098
C10B6	850	59	78	3.03	41014
C10B12	851	60	67	3.12	40426
C20B6	853	63	69	3.14	40132
C20B12	855	64	72	3.19	39718

Table 4: Orthogonal array design of experiment.

Exp. no.	Fuel	Load (%)	Speed (rpm)
1	Diesel type	0	1360
2	Diesel type	50	1380
3	Diesel type	100	1400
4	B10 type	0	1380
5	B10 type	50	1400
6	B10 type	100	1360
7	B20 type	0	1400
8	B20 type	50	1360
9	B20 type	100	1380

input–output pairs to operate with. Predictions can be made using the previously trained network on a new batch of data once the network has been trained. The input is break mean effective pressure (BMEP), injection timing, and engine speed (n), and exhaust temperature and brake specific fuel consumption (BSFC) are the outputs. The input and output values of a neural network must be between 0.1 and 0.9.

9. Result and Discussions

9.1. Analysis of Deposits on Polymer Surface. Biofuel fuel oxidation produces hydroperoxides, which break down and form low molecular weight compounds. Polymerization of tiny units produces heavy entities as well. A thin layer of residue forms on the polymer surface as a result of the breakdown and polymerization processes. The layer that forms is too thin and barely adheres to the surface, yet a soluble solvent dissolves it. After separating the solvent, the layer that can be easily studied. Ethanol and toluene are employed separately for various samples; there is no discernible difference between them, although the residues are sufficiently soluble in both.

9.2. Taguchi Optimization. The MINITAB-16 program was used to optimize the composite for optimal tensile strength and hardness. The results were obtained from the Taguchi orthogonal array studies on several materials by altering the reinforcement percentage, stirring speed, time, and temperature according to the Taguchi method. Figure 5 shows experiment versus hardness ratio which is illustrated in graphical representation and the values are listed in Table 5.

In Figure 6, experimental versus S/N ratio is illustrated in graphical representation. The comparison is done between experimental result and S/N ratio. The tensile strength (SN) and the hardness of the experimental and S/N ratio are compared. In experimental result, the tensile strength value is high compared to the S/N ratio, while in the other hand, the hardness is slightly variable in two processes. Hence, from the figure, we state that the tensile strength and the hardness are high in experimental value compared to the S/N ratio.

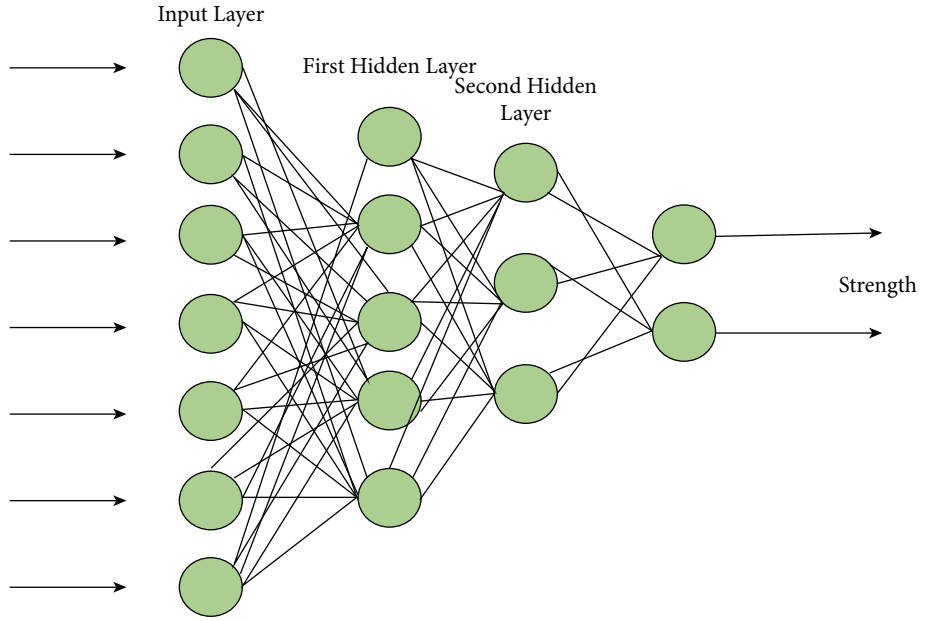

Figure 4: Model of ANN.

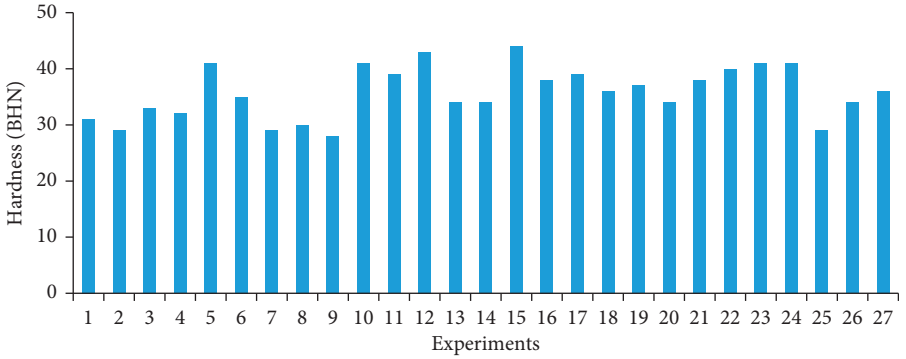

Figure 5: Taguchi optimization.

Table 5: Experimental and S/N ratio results.

Ex	TS (MPa)	Hardness (BHN)	S/N of tensile strength	S/N of hardness
1	71	30	37.7419	29.8272
2	72	29	37.1665	29.2480
3	79	33	38.1525	30.3703
4	76	32	37.6163	30.1030
5	77	41	37.3846	32.2557
6	74	35	37.3846	30.8814
7	74	29	37.5012	29.2480
8	73	30	37.2665	29.5424

10. Comparison between NO_x and Load for PPME Samples

Based on the tested fuel properties, the comparison between NO_x and load for PPME sample is calculated, and the graphical representation is given in the following.

In Figure 7, there is a comparison between the No_x and load for PMME; the graph is plotted against load and NOx in PPM; the load is literally high in 3rd stage when comparing to the other stages and only slight difference is found between each sample of PMME.

In Figure 8, there is a comparison between the No_x and load for CIME. The graph is plotted against load and NOx in PPM; the load is literally high in 3rd stage when comparing to the other stages, and only slight difference is found between each sample of CIME.

Figure 9 illustrates CO versus load for PPME samples. It is done at three stages and compared to one another. At first

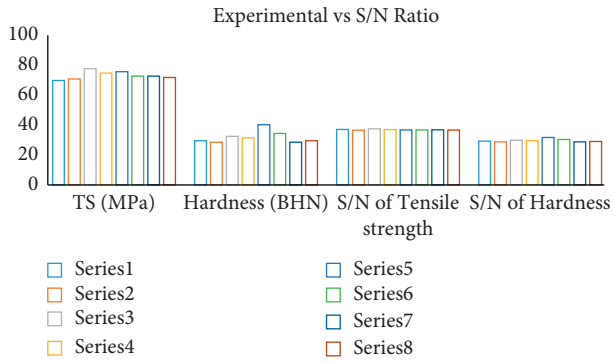

Figure 6: Experimental versus S/N ratio.

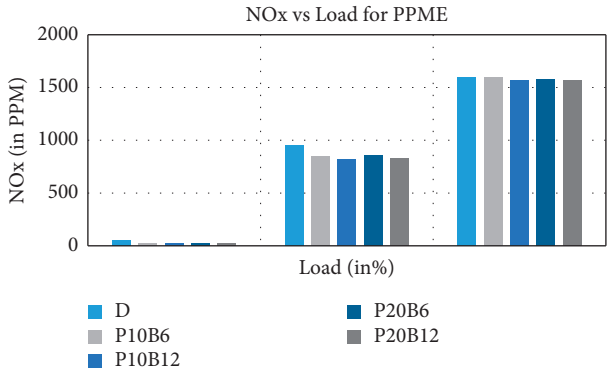

Figure 7: NOx versus load for PMME.

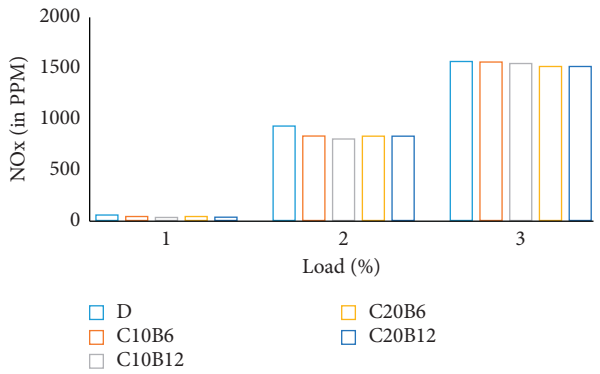

Figure 8: NOx versus load for CIME.

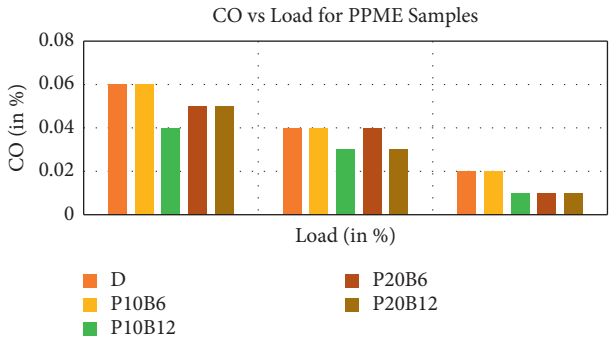

Figure 9: CO versus load for PPME Samples.

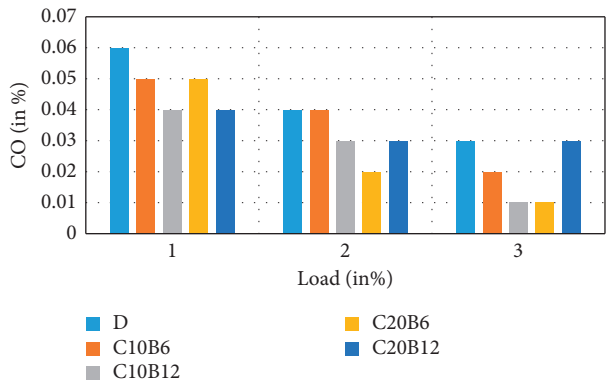

Figure 10: CO versus load for CIME samples.

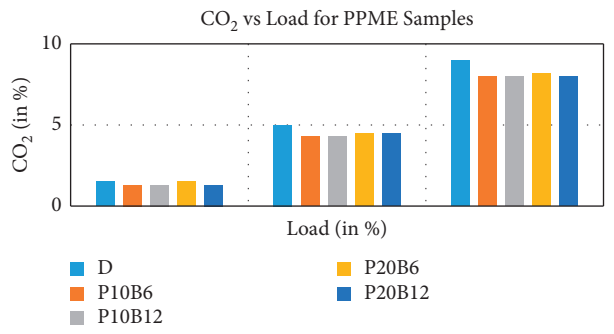

Figure 11: CO_2 versus load for PPME samples.

stage, *D* and P10B6 are high, compared to the other models, and in the second stage, *D*, P10B6, and P20B6 are equally high when compared to P20B12 and P10B12. In the final stage, *D* and P10B6 are equal, and P20B6, P10B12, and P20B12 are equal.

The CO versus load for CIME samples is illustrated in Figure 10; at the first stage, *D* is high when compared to other models. In the second stage, *D* and C10B6 are equal. In the final stage, when comparing to the other models, *D* and C20B12 are equal.

The CO_2 versus load for PPME samples is presented in Figure 11. At the first stage, all models or trails maintain an equal loading, and in the second stage, *D* is higher than the other models. In the final stage, *D* is high and the other models maintained an equal loading.

The CO_2 versus load for CIME samples is presented in Figure 12. At the first stage, all models or trails maintain a slight difference in loading, and in the second stage, C20B12 is higher than the other models. In the final stage,

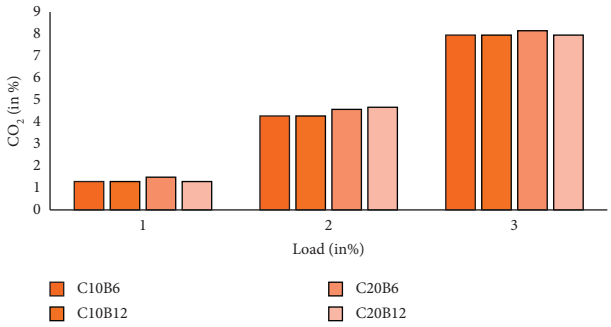

Figure 12: CO_2 versus load for CIME samples.

C20B6 is high, and the other models maintained an equal loading.

11. Conclusion

An artificial neural network architecture was constructed for predicting particular fuel consumption and exhaust temperature in a diesel engine. The effects of various composite casting parameters have been thoroughly investigated. Aside from stability, another advantage of polymer-coated reversed phases is the possibility to construct materials with a wide range of carbon loading. By combining evolutionary theory and natural swarm intelligence behaviors, hybrid PSO-GA algorithms create effective and usable data in less time than a thorough parametric investigation. Saving time lowers costs, making it easier to take advantage of innovative and proven techniques for improving engine performance. The performance of a diesel engine can be improved by using an artificial neural network (ANN), which saves time, money, and experimental repetition, due to the accuracy and the possibility of studying indiscriminately problems that will be solved by statistical and traditional ways by employing ANN. Even though it provides high accuracy, more time was taken for training purpose. This should be overcome in the future research.

Data Availability

The data used to support the findings of this study are included within the article.

Conflicts of Interest

The authors declare that there are no conflicts of interest regarding the publication of this article.

Acknowledgments

The authors would like to express their gratitude towards Saveetha School of Engineering, Saveetha Institute of Medical and Technical Sciences (formerly known as Saveetha University), for providing the necessary infrastructure to carry out this work successfully.

References

[1] T. K. Kotteda, R. B. R. Chekuri, B. Naga Raju, P. R. Kantheti, and S. Balakumar, "Analysis on emissions and performance of ceramic coated diesel engine fueled with novel blends using artificial Intelligence," *Advances in Materials Science and Engineering*, vol. 2021, Article ID 7954488, 13 pages, 2021.

[2] A. R. Studart, U. T. Gonzenbach, E. Tervoort, and L. J. Gauckler, "Processing routes to macroporous ceramics: A review," *Journal of the American Ceramic Society*, vol. 89, no. 6, pp. 1771–1789, 2006.

[3] R. M. Spriggs, "Applications and prospective markets for advanced technical ceramics," *Key Engineering Materials*, vol. 56-57, pp. 1–12, 1991.

[4] M. H. Ali, M. Rasul, M. Khan, N. Ashwath, and T. Rufford, "Emission characteristics of polymer additive mixed diesel-sunflower biodiesel fuel," *Energy Procedia*, vol. 156, pp. 59–64, 2019.

[5] I. Taymaz, K. Çakır, and A. Mimaroglu, "Experimental study of effective efficiency in a ceramic coated diesel engine," *Surface and Coatings Technology*, vol. 200, no. 1–4, pp. 1182–1185, 2005.

[6] M. M. K. Bhuiya, M. G. Rasul, M. M. K. Khan, N. Ashwath, A. K. Azad, and M. A. Hazrat, "Prospects of 2nd generation biodiesel as a sustainable fuel - Part 2: properties, performance and emission characteristics," *Renewable and Sustainable Energy Reviews*, vol. 55, pp. 1129–1146, 2016.

[7] A. Parlak, Y. Islamoglu, H. Yasar, and A. Egrisogut, "Application of artificial neural network to predict specific fuel consumption and exhaust temperature for a diesel engine," *Applied Thermal Engineering*, vol. 26, no. 8–9, pp. 824–828, 2006.

[8] M. P. Rigney, T. P. Weber, and P. W. Carr, "Preparation and evaluation of a polymer-coated zirconia reversed-phase chromatographic support," *Journal of Chromatography A*, vol. 484, pp. 273–291, 1989.

[9] M. V. S. M. Krishna, T. O. Prakash, P. Ushasri, N. Janardhan, and P. V. K. Murthy, "Experimental investigations on direct injection diesel engine with ceramic coated combustion chamber with carbureted alcohols and crude jatropha oil," *Renewable and Sustainable Energy Reviews*, vol. 53, pp. 606–628, 2016.

[10] T. H. Prasad, K. Hema Chandra Reddy, and M. M. Rao, "Performance and exhaust emissions analysis of a diesel engine using methyl esters of fish oil with artificial neural network aid," *International Journal of Engineering and Technology*, vol. 2, no. 1, pp. 23–27, 2010.

[11] N. A. Negm, M. A. Betiha, M. S. Alhumaimess, H. M. A. Hassan, and A. M. Rabie, "Clean transesterification process for biodiesel production using heterogeneous polymer-heteropoly acid nanocatalyst," *Journal of Cleaner Production*, vol. 238, Article ID 117854, 2019.

[12] H. Wang, S. Morando, A. Gaillard, and D. Hissel, "Sensor development and optimization for a proton exchange membrane fuel cell system in automotive applications," *Journal of Power Sources*, vol. 487, Article ID 229415, 2021.

[13] Y. Ö. Özgören, S. Çetinkaya, S. Sarıdemir, A. Çiçek, and F. Kara, "Artificial neural network based modelling of performance of a beta-type Stirling engine," *Proceedings of the Institution of Mechanical Engineers-Part E: Journal of Process Mechanical Engineering*, vol. 227, no. 3, pp. 166–177, 2013.

[14] T. W. Simpson, T. M. Mauery, J. Korte, and F. Mistree, "Kriging models for global approximation in simulation-

based multidisciplinary design optimization," *AIAA Journal*, vol. 39, no. 12, pp. 2233–2241, 2001.

[15] D. Wen and Y. Ding, "Effective thermal conductivity of aqueous suspensions of carbon nanotubes (carbon nanotube nanofluids)," *Journal of Thermophysics and Heat Transfer*, vol. 18, no. 4, pp. 481–485, 2004.

[16] K. Viswanathan, W. Wu, M. I. Taipabu, and W. Chandra-Ambhorn, "Effects of antioxidant and ceramic coating on performance enhancement and emission reduction of a diesel engine fueled by Annona oil biodiesel," *Journal of the Taiwan Institute of Chemical Engineers*, vol. 125, pp. 243–256, 2021.

[17] J. Sharaf, "Exhaust emissions and its control technology for an internal combustion engine," *International Journal of Engineering Research and Applications*, vol. 3, no. 4, p. 14, 2013.

[18] L. Dobrzański, M. Staszuk, and R. Honysz, "Application of artificial intelligence methods in PVD and CVD coatings properties modelling," *Archives of Materials Science and Engineering*, vol. 58, no. 2, pp. 152–157, 2012.

[19] S. Fidan, H. Oktay, S. Polat, and S. Ozturk, "An artificial neural network model to predict the thermal properties of concrete using different neurons and activation functions," *Advances in Materials Science and Engineering*, vol. 201913 pages, 2019.